

# nFacet 3D: Fission Neutron Measurements With A Segmented Scintillation Detector

Nicholas Reed<sup>1</sup>, Anders Axelsson<sup>2</sup>, Gerald Kirchner<sup>3</sup>, Sakari Ihantola<sup>4</sup>, Manuel Kreutle<sup>3</sup>, Kari Peräjärvi<sup>4</sup>, and Antonin Vacheret<sup>1</sup>

<sup>1</sup>Imperial College London, Department of Physics, London, United Kingdom

<sup>2</sup>Swedish Radiation Safety Authority (SSM), Sweden

<sup>3</sup>University of Hamburg, Hamburg, Germany

<sup>4</sup>Radiation and Nuclear Safety Authority (STUK), Finland

## Abstract

nFacet 3D is a segmented scintillator detector capable of multi-mode detection of gammas, neutrons and muons. As a result of the detector segmentation, it is possible to sample the radiation field direction and energy. The system has therefore both location and source identification capabilities, which are both desirable for tracking nuclear material in various contexts. As a part of the 2019 International Partnership for Nuclear Disarmament Verification (IPNDV) measurement campaign, the system was deployed at the Belgian Nuclear Research Centre (SCK CEN) to take measurements of mixed-oxide (MOX) fuel assemblies. This exercise aimed to test the system in a realistic environment, including measuring in an indoor environment with a challenging background. We report in this paper the results obtained in neutron mode for the neutron fluence measurements and comparison with simulation. We report successful measurements of background and neutron source directions, sensitivity to the MOX-fuel assemblies neutron energy in different shielding configurations and a test of imaging the assembly geometry which was found to be inconclusive. We briefly present at the end, recent developments on neutron scattering and gamma-ray measurements which may extend the capabilities of the nFacet 3D detector in a future exercise.

## 1 Introduction

### 1.1 The nFacet 3D detector

The nFacet 3D detector is a novel segmented scintillation detector optimised primarily for neutron capture, made up of 64 polyvinyl toluene (PVT) cubes arranged in a 4 x 4 x 4 lattice. Each cube has a <sup>6</sup>LiF:ZnS(Ag) screen on three of its six faces, with wavelength shifting fibres set into grooves along each cube. The signal from each fibre is read out by a 3 x 3 mm square SiPM from Hamamatsu. The detector weighs 16 kg and measures 25 x 25 x 27 cm<sup>3</sup>, with a photograph of the system visible in Figure 1.

Whilst the detector is sensitive to both gamma rays and neutrons, in this exercise we operated only in neutron trigger mode. Incident neutrons thermalise in the PVT, before capturing on the <sup>6</sup>LiF:ZnS(Ag) screens. The decay to an alpha particle and a triton causes subsequent excitation and emission of UV scintillation photons in the ZnS(Ag). The scintillation

light is collected by two wavelength shifting fibres (one in each of the X and Y directions) providing spatial localisation of the photon signals. The SiPM signal waveforms are collected at the end of the fibre and digitised at 33 MS/s using custom electronics designed for the system.

The segmentation in voxels enables neutron field characterisation and source localisation. Measurements of neutron count attenuation in the longitudinal direction provide energy sampling. The vector direction of attenuation, measured through the transverse segmentation, enables source localisation. As a result, three-dimensional segmentation provides both full field characterisation and source localisation. With the current data acquisition system, the detector can register a maximum neutron flux of up to  $10 \text{ n/s/cm}^2$  on the face before saturation.



Figure 1: The nFacet 3D detector.

## 2 Lab Reference Measurements

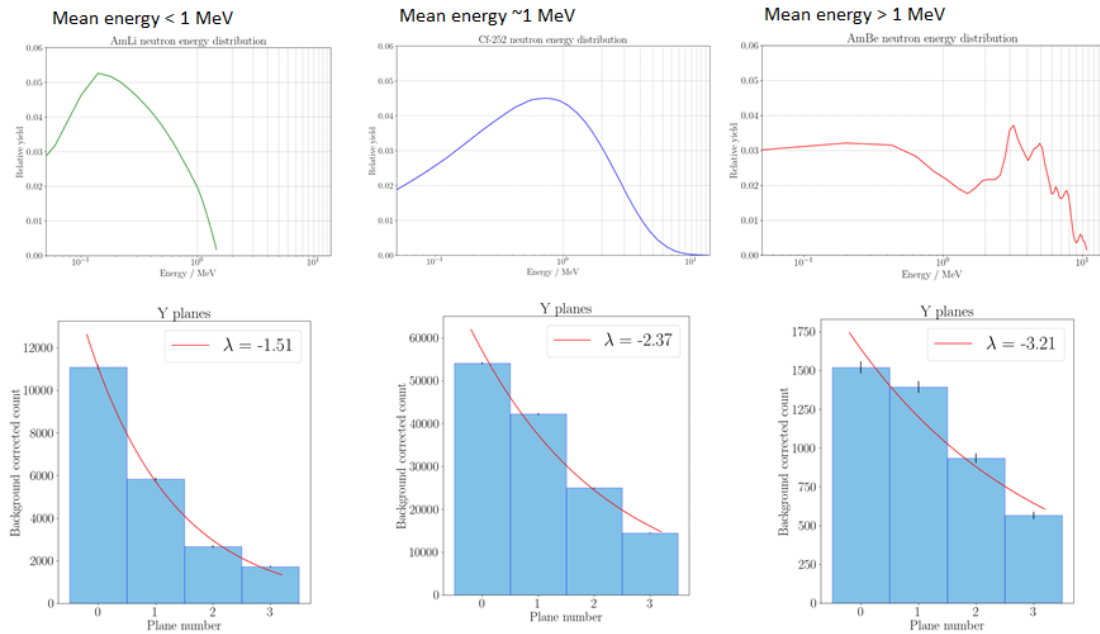


Figure 2: Count profiles for NPL fission sources.

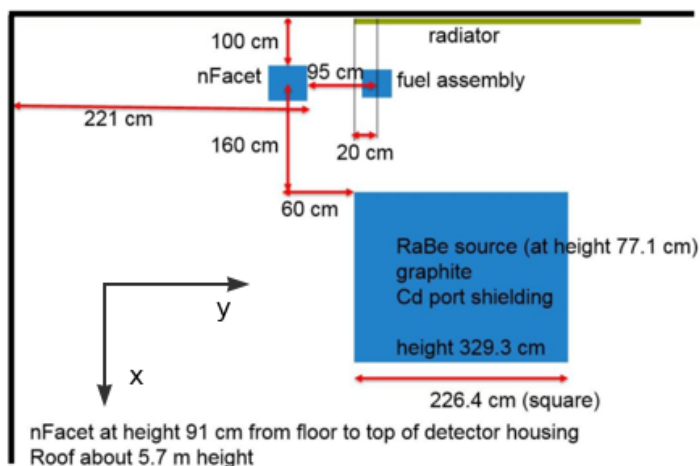
In 2017, a series of reference measurements were made at the low-scatter facility of the National Physical Laboratory (NPL) in Teddington, UK. This enabled the system to be tested in a controlled environment, gathering useful reference data with limited scattering. Various neutron sources were measured, including  $^{252}\text{Cf}$ , AmBe and AmLi, giving a good range of mean neutron energies. To demonstrate the level of source discrimination, the neutron count in planes facing the source across the detector is used to create a profile of stopping power. This is illustrated in Figure 2. A first order model based on a decaying exponential is used to fit each source profile to characterise the average attenuation in plane

lengths. Even from this simple metric, there is a marked difference in the count profile for each of the different average energy values. These results motivates the development of a more sophisticated inversion method for fluence characterisation as implemented with other neutron survey meters or Bonner sphere systems.

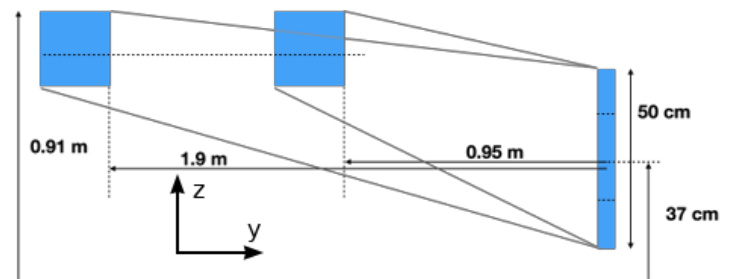
### 3 The IPNDV exercise at SCK CEN



(a) A photo of the nFacet 3D system on a tripod ready to take data with the MOX assembly in front.



(b) Top down schematic of the nFacet 3D IPNDV setup at SCK CEN.



(c) Details of the nFacet 3D distance and heights from the assemblies position. Measurements were made at two different distances, 0.95 m and 1.9 m.

Figure 3: The experimental setup at SCK CEN.

The detector was set up to measure neutron fluence from mixed-oxide (MOX) fuel assemblies, bare and with additional shielding, at the Belgian Nuclear Research Centre (SCK CEN) to understand what can be learned from nFacet 3D system measurements. This deployment constituted one of the first tests of the nFacet 3D system in a real-life scenario with a challenging background and was therefore an important step also in demonstrating the robustness of the technology. Count rate measurements were recorded with and without the MOX assembly present, to characterise responses to the background and the source separately. The recorded neutron count rates across cubes was used to infer the direction to the source. The rate profile of the MOX assembly was compared with the NPL  $^{252}\text{Cf}$  fission measurements. Two detector orientations, at  $0^\circ$  and  $90^\circ$ , were used to assess the angular dependence of the detector response. Measurements of two different assemblies were made, ID 79-19 and ID 96-19, which consisted of 79%  $^{239}\text{Pu}$  and a mixture of 96%  $^{239}\text{Pu}$

and 79%  $^{239}\text{Pu}$  respectively. Both assemblies were measured at different distances due to a large difference in neutron activity (at 1.9 m for ID 79-16 and at 0.95 m for ID 96-16). The detector was at a height of 0.91 m from the ground, slightly off axis of the MOX assembly centre which was at a height of 0.37 m. A photo and two schematics of the setup are shown in Figures 3a, b and c. A variety of shielding configurations were studied as a part of the exercise, including Cd and  $\text{CH}_2 + \text{Pb}$ .

Prior to the MOX assembly measurements, neutron background data was recorded. The cube-level data for this survey is shown in Figure 4. The background measured consisted of a directional RaBe pile component and a diffuse component from assemblies in adjacent rooms. A background neutron rate of approximately 51 Hz was measured at both distances, resulting in a signal to background ratio of 2:1. This complex background is expressed in the detector, with a large component incident on one edge originating from the pile, identified as thermal neutrons due to a lack of detector penetration. The remaining signal is due to scattered neutrons in the room, which produce small counts incident on other faces.

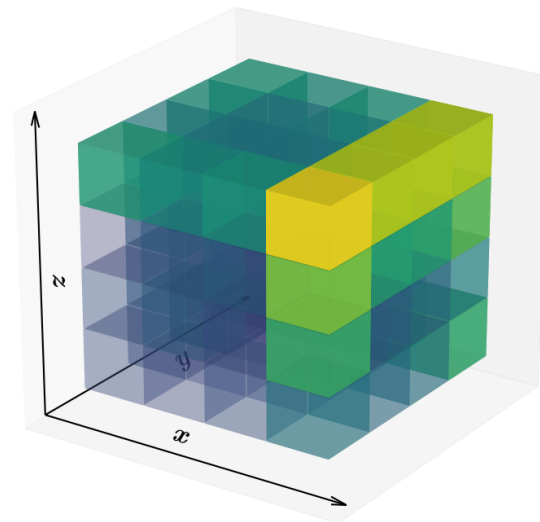


Figure 4: Individual voxel cube rates for background data showing localised and directional neutron background.

## 4 Results

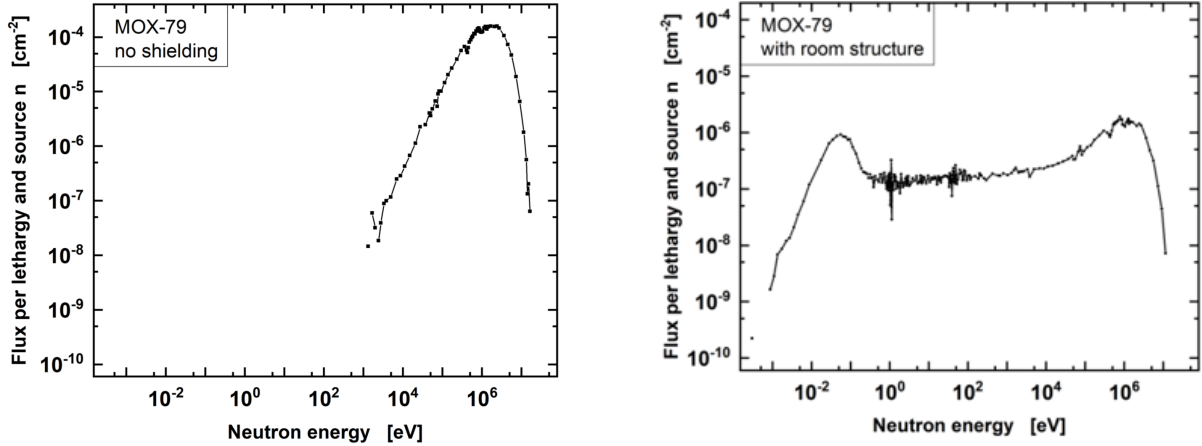
### 4.1 Direct and scattered rates

To characterise the direct and scattered components of the neutrons incident on the detector, neutron flux densities and energy spectra for the 79%  $^{239}\text{Pu}$  MOX assembly were simulated by G. Kirchner and M. Kreutle. The simulation was based on the SCALE code system and the ENDF/B-VII database, and calculation of rates was done using the KENO Monte Carlo code. The simulation included the floor, walls and the RaBe pile in the middle of the room providing accurate estimation of the complex neutron scattered component. Expected and measured rates on the face of nFacet 3D from the 79%  $^{239}\text{Pu}$  assembly are shown in Table 1 alongside expected rates from a point source of the same isotopic composition. Measurements were made at 1.9 m for the bare 79% source as the system could not register the total rate at 0.95 m. From Geant4 Monte Carlo simulations of the detector the expected efficiency of capture for a bare fission source is  $\sim 0.25$ , whilst the measured efficiency is only 0.19. Due to the high rate at SCK CEN a higher threshold trigger was used to keep the system from saturating, reducing the measured neutron rate by  $\sim 20\%$  and thus reducing the measured efficiency. The measured efficiency is further reduced by channel-to-channel response differences in the detector. The  $\text{CH}_2$  shielding scatters a greater proportion of the emitted neutrons, resulting in a larger near-thermal component incident on the detector and thus resulting in a greater measured efficiency for this configuration. The simulated and measured rates are consistent with each other and with the known nFacet 3D efficiency. The simulated rates also show that a large fraction of the detected rate is due to scattered

neutrons incident on the face of the detector. This is further illustrated in the difference between the simulated emitted flux and the flux entering the detector, as shown in Figures 5a and 5b respectively. The low energy component in the flux entering the detector is due to scattering in the room.

Assembly	79%			96%	
Neutron activity [Bq]	93000			37000	
Distance L [m]	0.95	1.9	0.95		
Point source on face [Hz]	328.0	86.5	130.5	34.4	
Shielding	Cd	CH <sub>2</sub>	Bare	Cd	Bare
KENO sim rate on face [Hz]	595±2	237±1	312±1		
KENO no scatter [Hz]	267	112	81		
nFacet rate [Hz]	112	101	59	51	55
Measured efficiency	0.19	0.42	0.19		

Table 1: Table of simulated rates compared with the measured nFacet 3D rate. When accounting for detector efficiency, the simulation is consistent with the measured rates.



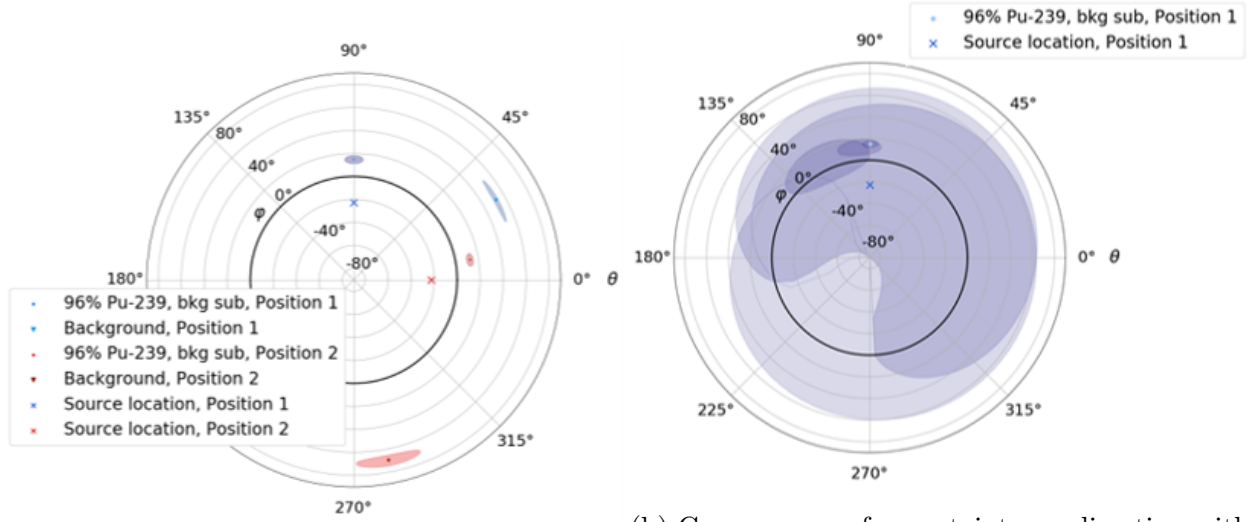
(a) Simulated flux emitted from the ID 79-19 MOX assembly at SCK CEN.

(b) Simulated flux entering the detector from the ID 79-19 MOX assembly at SCK CEN, accounting for scattering in the room.

Figure 5: Simulated flux emitted and entering the detector from the ID 79-19 MOX assembly at SCK CEN.

## 4.2 Direction reconstruction

Two main direction reconstruction results were obtained from the large samples of cube neutron rates collected. Firstly, the direction to the source was reconstructed by fitting a three-dimensional direction vector to the cube rate distribution. Figure 6a shows the reconstructed directions, comparing the data after background subtraction. The crosses indicate the true direction to the MOX assemblies in each position. The angular coordinate  $\theta$  indicates angle in the x-y plane, whilst the radial coordinate  $\phi$  is the angle made to the x-y plane. The shaded region around each data point indicates the 99.7% ( $3\sigma$ ) confidence interval in each direction. The true direction of each source has a  $\phi$  angle value less than  $0^\circ$



(a) Direction reconstruction for two positions, with and without the MOX assembly. (b) Convergence of uncertainty on direction with increasing neutron count for 10, 100, 1000, 10000 and 100000 neutrons, where the largest region has 10 neutrons and the smallest has 100000.

Figure 6: Direction reconstruction and convergence of uncertainty on reconstructed direction for the IPNDV exercise.

as the detector was at a higher position than the assembly.

At position 1 the  $\theta$  angle matches the expected value, but in both positions the  $\phi$  angle is significantly far from the true position of the source. This discrepancy, and the error in the  $\theta$  angle at position 2, are attributed to two different factors. A first contributing factor to the  $\phi$  angle is the difference in height between the detector and the source, leading to a larger acceptance for lower cubes than higher ones. In future measurements this effect will be better characterised by testing varying relative heights of source and detector. The second contributing factor is the  ${}^6\text{LiF}:\text{ZnS}$  screen placement on the detector cube faces; this creates a slight bias in the position of capture, translating into a directional reconstruction bias.

It is also informative to see how the uncertainty in direction reconstruction converge as the total neutron count increases, as shown in Figure 6b. Each shaded region indicates the 99.7% confidence region for the reconstructed direction with different amounts of neutrons. The figure shows that after 10,000 neutrons, the reconstructed direction is accurate to within  $10^\circ$ . At typical source rates, the mean direction can be reconstructed at the level of a few degrees in minutes, even with a simple algorithm.

### 4.3 Source profiles

The data collected is also useful to compare with the source characterisation discussed in Section 2. By fitting the same decaying exponential model to the planes facing the MOX assembly, the average attenuation length  $\lambda$  can be compared with thermal, fast neutron and fission datasets for each configuration, as shown in Figure 7. This shows that this metric is consistent with that of a fission source for the unshielded and Cd shielded configurations, whilst it is more consistent with a thermal source for the  $\text{CH}_2 + \text{Pb}$  shielded configuration. Despite the large scattering component identified in section 4.1, the system is capable of separating thermal, fission and high energy neutron sources. A more precise method will be

developed to investigate the sensitivity to neutrons from  $(\alpha, n)$  reactions.

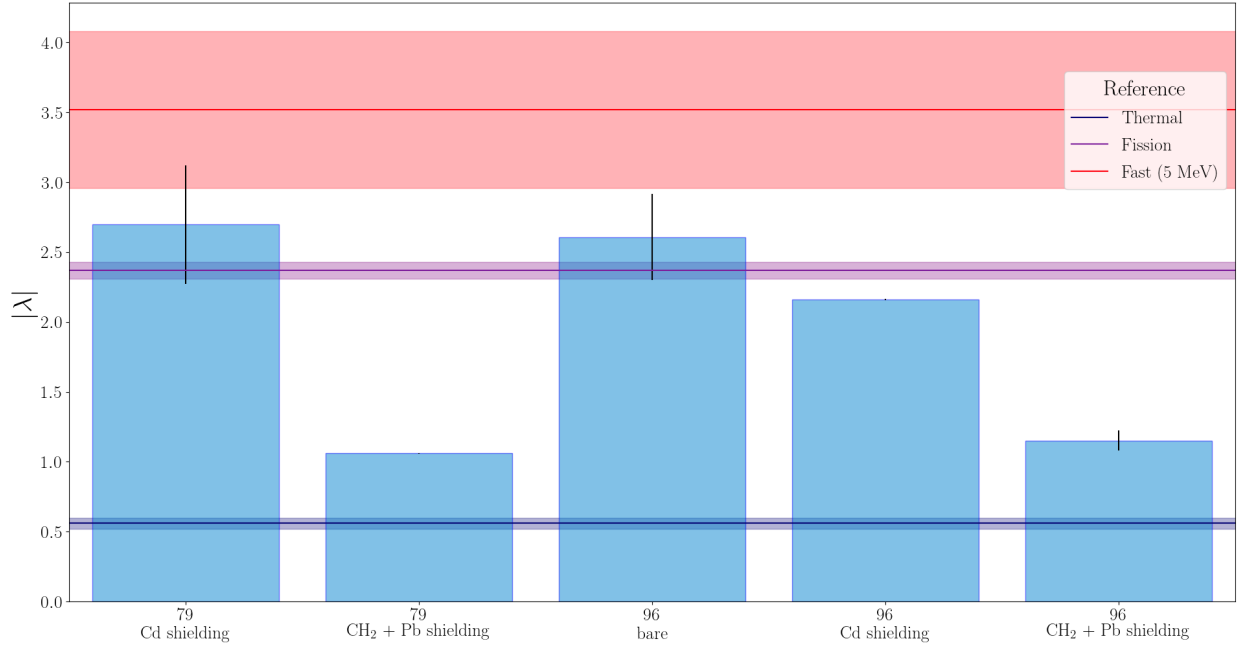
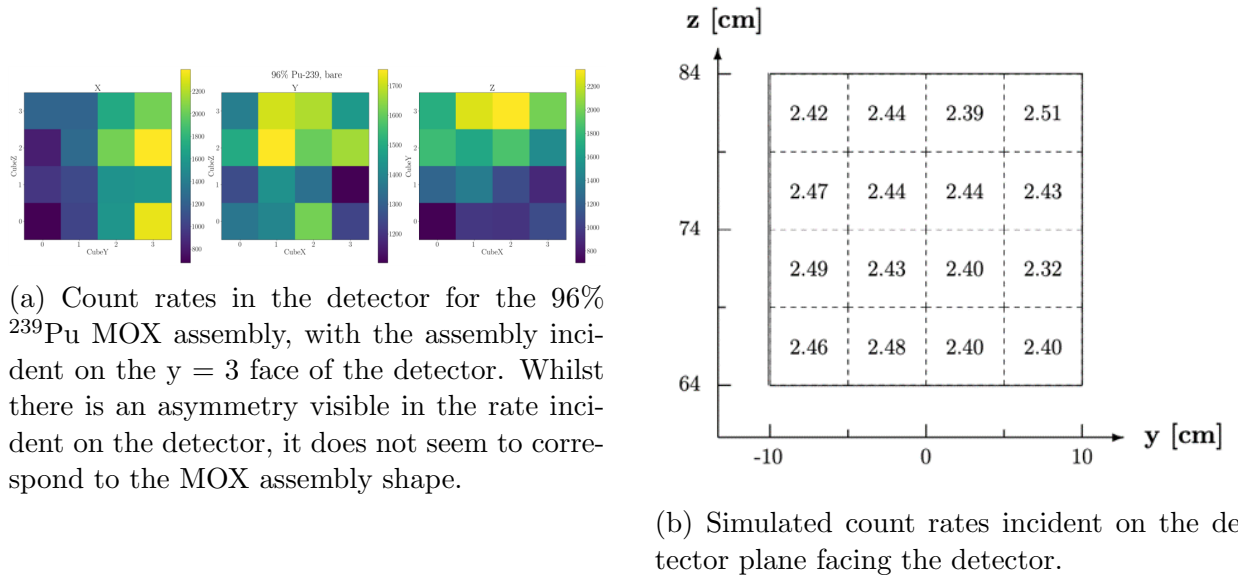


Figure 7: Characteristic attenuation length in plane count for various sources. The bare 96% and Cd shielded 79% are clearly similar to the fission source. The black vertical lines indicate the uncertainty on the attenuation length, whilst the shaded regions indicate the uncertainty on the reference values. The fission reference is calculated from the lab reference measurements described in Section 2, whilst the thermal and high energy data was produced via Geant4 Monte Carlo simulations of the detector.

#### 4.4 Geometry of the source



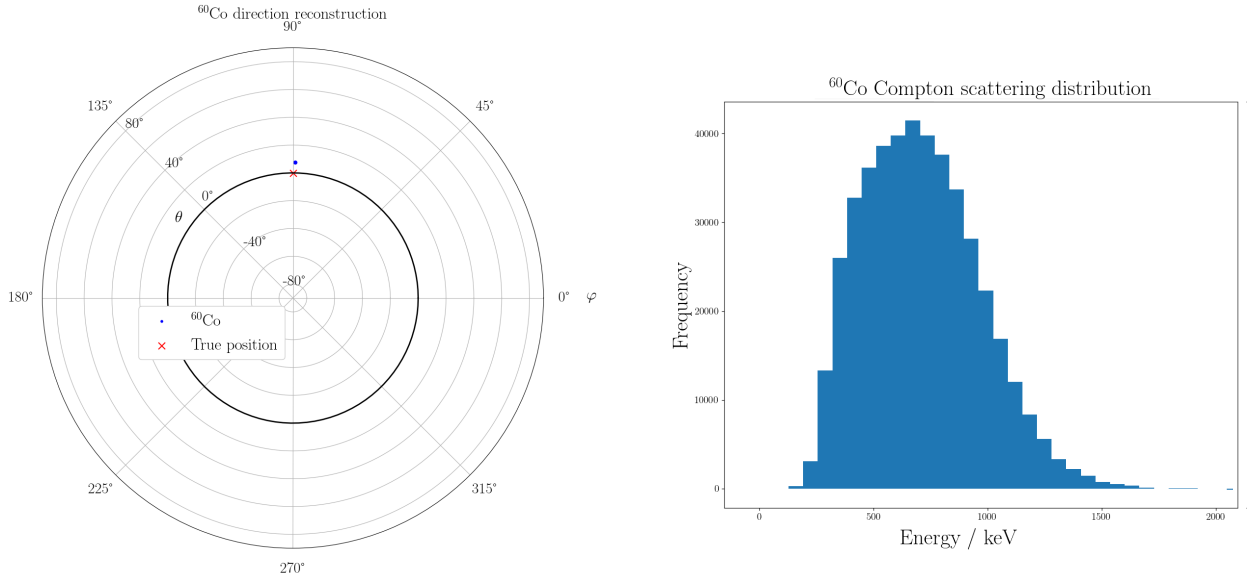
(a) Count rates in the detector for the 96%  $^{239}\text{Pu}$  MOX assembly, with the assembly incident on the  $y = 3$  face of the detector. Whilst there is an asymmetry visible in the rate incident on the detector, it does not seem to correspond to the MOX assembly shape.

(b) Simulated count rates incident on the detector plane facing the detector.

Figure 8: Real and simulated rates on the detector with the 96% MOX assembly. Neither shows a pattern corresponding to the MOX assembly shape.

It is also important to verify if the system can measure the shape of the neutron source. From the distribution of counts across the detector cubes, we can see both from the measured data and the simulated rates that there is no easily discernible pattern in the count distribution that could correspond to the source shape, as seen in Figures 8a and 8b. The detector spatial resolution seems too coarse to provide useful measurement of the source shape, which could be an advantage in a nuclear verification context.

## 5 Other capabilities of the nFacet 3D detector



(a) Direction reconstruction of a  $^{60}\text{Co}$  source. As the direction reconstruction only relies on the distribution of counts across detector cubes, the direction can be reconstructed in the same way as for neutrons.

(b) The Compton scattering distribution for a  $^{60}\text{Co}$  source, as measured by the nFacet system. The  $1\sigma$  spread is at the first Compton edge energy of 960 keV.

Figure 9: Direction reconstruction and Compton scattering distribution for a  $^{60}\text{Co}$  source.

Whilst the system was only deployed in neutron mode at SCK CEN, it is also capable of performing gamma measurements, with a different trigger. The same direction reconstruction analysis for neutrons can be applied for gammas, as it only relies on the geometry of the system. An example of this reconstruction can be seen in Figure 9a, for a  $^{60}\text{Co}$  source. The system is also capable of recording the Compton scattering distribution of a gamma source, as shown in Figure 9b, again for a  $^{60}\text{Co}$  source. Further analysis of the gamma measurement capabilities of the system is ongoing.

The system is also capable of measuring both neutron scatter and capture on  $^6\text{Li}$  to better characterise incident neutrons. Running in a gamma trigger mode, scatter events are recorded as gamma signals and then paired with coincident neutron signals, with the time between signals following a characteristic exponential decay determined by the average scattering time in the detector, of the order of  $50\ \mu\text{s}$ . This is illustrated in Figure 10.

As discussed previously, a sophisticated inversion method is required for full source characterisation. Currently, a neural network approach to reconstruct the source fluence is under development. Initial tests seem promising, but further development is required.



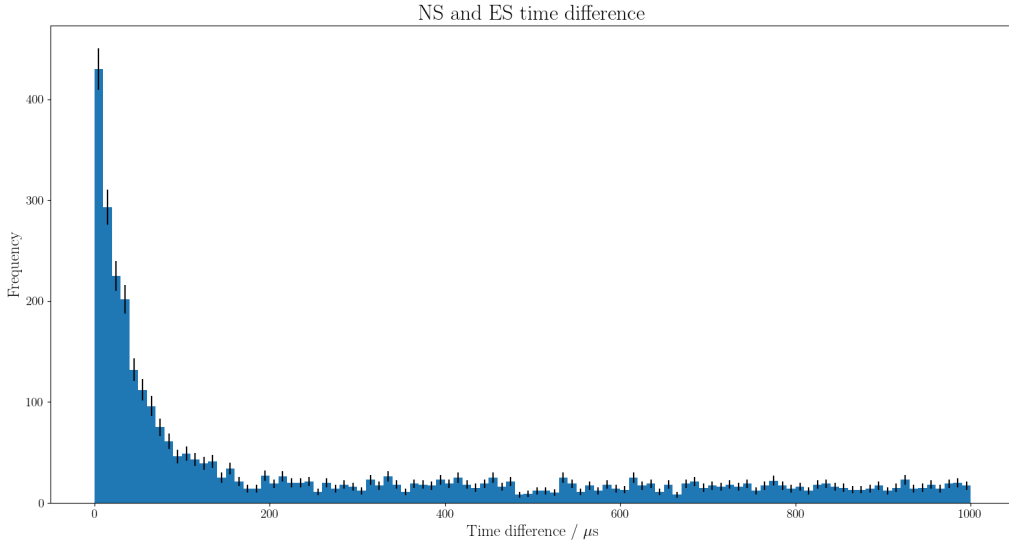


Figure 10: Time difference between coincident gamma and neutron signals. This shows an exponential decay from scatter + capture events, on top of a flat accidentals component.

## 6 Conclusions

The IPNDV exercise was a successful test of the nFacet 3D detector in real conditions. A useful dataset of MOX assemblies was collected, direction reconstruction capabilities were demonstrated, and source geometry imaging was tested. A semi-quantitative measurement of neutron fluence was demonstrated, with development of more sophisticated methods ongoing. Some key areas for improvement were also identified, including compensating for neutron count biases in the detector, extending measurements to higher neutron source activity and to both gammas and neutron scatter events.

There are several key takeaways from this exercise. This campaign has been sufficient to understand neutron measurement based on  ${}^6\text{Li}$  capture, verifying that simple source identification and direction reconstruction can be performed in realistic conditions. Source identification was found to be robust even in the presence of a large scattered component. The high sensitivity of the system can result in difficulties registering high rates, unless operated at lower efficiency or at greater distances.

Measurements in this environment for additional analyses would have been useful, such as  ${}^{252}\text{Cf}$  measurements, to compare with lab condition reference measurements. Additionally, data taken in a gamma trigger mode for dual gamma-neutron and elastic scattering analyses would allow more detailed source characterisation.